



Cite this: *Chem. Commun.*, 2021, 57, 3765

Received 5th February 2021,
Accepted 8th March 2021

DOI: 10.1039/d1cc00704a

rsc.li/chemcomm

Scalable synthesis and purification of functionalized graphene nanosheets for water remediation†

Sebastiano Mantovani,^a Sara Khaliha,^a Laura Favaretto,^a Cristian Bettini,^a Antonio Bianchi,^a Alessandro Kovtun,^a Massimo Zambianchi,^a Massimo Gazzano,^a Barbara Casentini,^b Vincenzo Palermo^a and Manuela Melucci^a

Microwave (MW) accelerated synthesis combined with microfiltration (MF) on commercial hollow fiber modules enables fast and scalable preparation of highly pure modified graphene oxide nanosheets. The MW–MF procedure is demonstrated on polyethylenimine (PEI) modified GO, and the so-obtained GOPEI is used for simultaneous removal of arsenic and lead from water.

Covalent modification of graphene oxide is a widely exploited and powerful strategy to tune the surface properties, packing and structure of GO sheets in order to achieve new functionalities for applications spanning from energy, sensing to biomedical and environmental remediation fields.¹ Modified GO nanosheets can be prepared by exploiting the multiple oxygenated surface chemical groups of GO including carboxylic, hydroxyl and epoxide functionalities by conventional synthetic pathways such as amide coupling (on activated COOH), epoxide ring opening or nucleophilic substitution of OH groups.^{2,3}

In recent years, a plethora of modified GO have been engineered and proposed as specific sorbent materials for water purification^{4–9} from organic and metallic contaminants. Indeed, enhanced adsorption of heavy metal ions such as Cu²⁺ and Pb²⁺, and organic dyes such as methylene blue, in water and wastewater has been reported using EDTA,¹⁰ sulphonate¹¹ and amino modified GO.¹²

Among them, of particular relevance is the branched cationic polyethylenimine (PEI), modified graphene oxide (GOPEI).^{13,14} Branched PEI is a water soluble positively charged polyelectrolyte, containing primary, secondary and tertiary amino groups with demonstrated chelating properties with various metal ions.¹⁵ The effectiveness of GOPEI porous foams was recently demonstrated

in the removal of metal cations including Pb(II) from aqueous solutions with the maximum uptake capacity in the range of 1096–3390 mg g^{−1}, *i.e.* 20 times greater than that of activated carbons.¹³ Moreover, GOPEI modified cellulose fibers have been exploited for the preconcentration of trace arsenate and arsenite under selected pH conditions.¹⁶

It is noteworthy that lead and arsenic are the two contaminants of actual concern¹⁷ included in the newly adopted drinking water directive EU 2020/2184 which tightened the limit admitted for lead, calling for the development of more efficient purification technologies.

However, real exploitation of modified GO for water purification requires large availability of materials^{18a,b} and a high and reproducible batch purity level to avoid secondary contamination caused by leaching of not-covalently bonded reagents and to guarantee reliable and stable batches performances.

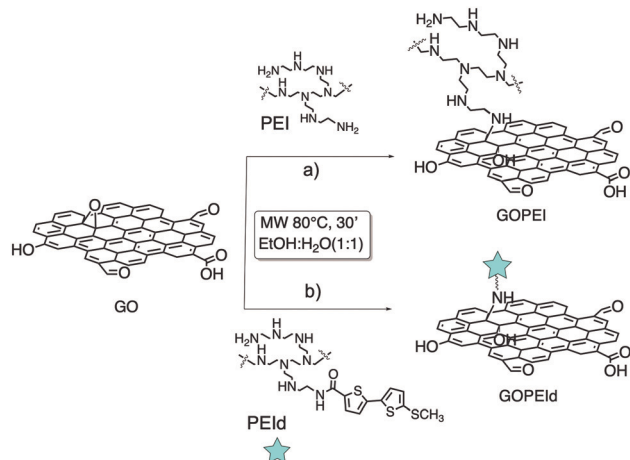
To this aim, here we report a new approach based on microwave (MW) assisted synthesis combined with microfiltration (MF) on commercial hollow fiber modules (Fig. S1, ESI†), allowing fast modification and efficient-reproducible purification of GO. The rationale behind the MF method relies on the peculiar structure of the module polymeric core, consisting of porous hollow fibers (Versatile PES, Medica SpA) with a cut-off value in the range of 100–200 nm. Due to such a cut-off value, the module can stop objects larger than the pore size while allowing the permeation of smaller species such as reaction side-products including unreacted molecules. Given its already highlighted performance in water treatment, GOPEI was selected as a case study. GO and PEI suspension in water–EtOH was irradiated with MW at 80 °C at a fixed power of 120 W for 30 minutes rather than refluxed for 24 hour under conventional heating as previously described (Scheme 1a).¹³ The same protocol was exploited to synthesize a fluorescent analogue (GOPEId) that is used to monitor the evolution of the purification in the following MF step. To this aim, we used a blue emitting thiophene based dye functionalized with a succinimidyl end group¹⁹ that spontaneously reacts with the amino moieties

^a Institute of Organic Synthesis and Photoreactivity (CNR-ISOF) Via Piero Gobetti 101, 40129, Bologna, Italy. E-mail: manuela.melucci@isof.cnr.it

^b Consiglio Nazionale delle Ricerche–Water Research Institute (CNR-IRSA), Via Salaria Km 29,300 C. P. 10-00015, Italy

† Electronic supplementary information (ESI) available: Microfiltration module structure, synthesis, PEI loading estimation, ATR-FTIR, XPS, XRD, and contact angles. See DOI: 10.1039/d1cc00704a





Scheme 1 Synthetic pathways to GOPEI and GOPEId.

of the branched PEI (Fig. S2, ESI[†]). Then, the crude material was purified by MF on commercial Versatile PES[®] hollow fiber modules (Plasmart, Medica SpA) in dead-end filtration modality (in-out), *i.e.* by forcing the solution to pass through the hollow fiber membrane section through a peristaltic pump (Fig. 1).

The suspension was introduced into the fiber lumen and forced to exit by the outer surface after passing through the section. In this modality (called dead-end in-out mode), the GOPEI sheets could not pass through the fiber pore and remain staked on the inner fiber surface. This was demonstrated by the filtered solution which was clear (Fig. 1d).

Once immobilized on the inner fiber wall, the GOPEI sheets were washed with MilliQ water: EtOH solution, until no PEI (or PEId) was detected in the eluted water fractions (Fig. 1(e) and (h)). The monitoring of PEI in the washing water fractions was performed using UV-vis spectroscopy after complexation with copper salts (absorption peak of the Cu-PEI complex at 277 nm) according to already known protocols (Fig. S3 ESI[†]).¹¹ Moreover, for further confirmation we performed the same protocol on GOPEId. The eluted fractions showed intense blue fluorescence until all the unreacted PEId was separated (Fig. 1e and h).

Besides the online fluorescence monitoring (Fig. S4b, ESI[†]) we performed UV-vis spectroscopy on the collected fractions (Fig. S4b, ESI[†]) and monitored the lowering of the absorbance peak of the PEId located at about 350 nm.

Due to the separation intrinsically allowed by the microfiltration mechanism, we were able to collect all the unreacted PEI and estimate the degree of PEI loading by (i) complexation with copper, (ii) monitoring the PEId absorbance during

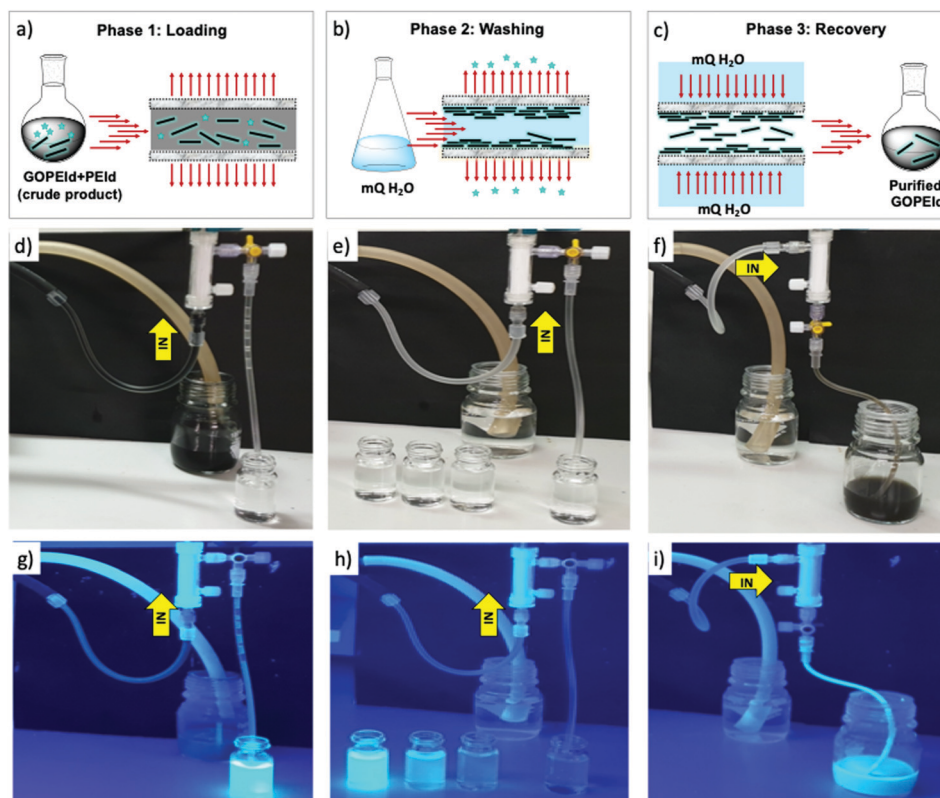


Fig. 1 Sketch of the microfiltration procedure (Plasmart 25 cartridge, Medica spa) and images of the real set-up by using PEId to visually monitor the evolution of the purification. (a) Loading phase: the crude suspension is introduced into the hollow fibers passing each fiber from in to out, (b) washing phase: the immobilized GO sheets are washed with MilliQ water in the same flow direction (in-out) and (c) recovery phase: purified GOPEId is collected in the opposite flow direction (out-in). (d–f) Experimental set-up under normal light corresponding to each phase and (g–i) same experimental set-up under UV light ($\lambda = 365$ nm) showing the evolution of the fluorescence during each phase.



elution and (iii) by the weight of the evaporated eluted fractions. According to both procedures, a loading of PEI of about 40% was achieved and about 2.5 L of water were required to purify 1 gram of crude GOPEI.

The estimated loading was confirmed also by thermogravimetric analysis (TGA, Fig. S5, ESI[†]) and XPS.

Finally, the washed GOPEI sheets were collected by flowing water in the direction opposite to that of the loading phase (Fig. 1c, f and i) and a total reaction yield of 63% in GOPEI was achieved.

The ATR-IR spectra of GOPEI (Fig. S6, ESI[†]) showed the typical fingerprint of GO and the appearance of PEI aliphatic chain peaks in the range of 2850–2950 cm^{-1} .

X-Ray photoelectron spectroscopy (XPS) revealed the increase of nitrogen (N 1s) in GOPEI from 0.9% for GO to 10.4% for GOPEI, confirming the presence of PEI chains.

Moreover, the amount of PEI could be roughly estimated considering that XPS showed about 10 atoms of N in every 100 atoms of GOPEI; the PEI has a C:N ratio of 2, thus, approximately 30% of atoms in GOPEI can be associated with PEI, in good accordance with post-microfiltration experiments and TGA. The representative morphologies of GOPEI are shown in Fig. 2b. GOPEI shows sheets resembling the mesoscopic structure of GO typical sheets, but with amorphous structures at the edge of the sheets probably due to the branched PEI chains. XRD of GOPEI sheets showed the loss of sharp reflection of GO patterns at 10.5° due to the (001) interlayer distance $d = 0.84$ nm (Fig. S7, ESI[†]). The successful grafting of PEI was also confirmed by Z potential measurements. The negative surface charge of GO with (Z potential = -23.2 mV) becomes positive after PEI grafting in GOPEI (Z potential = 14.9 mV). Also, the wettability of GOPEI sheets changed with respect to GO due to the binding of the hydrophilic PEI chains. Indeed, the water contact angles of the prepared multilayer membranes of GO and GOPEI (prepared by vacuum filtration of GO/GOPEI suspension on PES support, details in the ESI[†], Fig. S8) were measured and revealed higher hydrophilicity for GOPEI (GOPEI $\theta = 30.9^\circ$ and GO $\theta = 38.5^\circ$). Microwave-microfiltered (MW-MF) prepared GOPEI was then used as a sorbent for arsenic and lead contaminants, simultaneously from spiked tap water ($\text{pH} = 7 \pm 0.5$) at an environmentally relevant concentration ($100 \mu\text{g L}^{-1}$ each).

Fig. 3 shows the removal kinetics of the adsorption for GOPEI in comparison to GO. A 97.6% removal rate has been achieved using GO for Pb removal after only 10 min, due to its high affinity on the negatively charged surface at experimental pH (GO pH_{pzc} is around 2) and As adsorption was only 10% at 10 min with a decreasing trend (1% at 24 h), due to the anionic form in which arsenate is present at circumneutral pH (Fig. 4a). PEI modification provided, at this pH, a shift towards more positive surface charges, mainly driven by the protonation of amino groups in branched PEI at this pH,²⁰ therefore, we observed an increase in As adsorption up to 49.1% after 10 min (87.5% at 24 h) and simultaneous Pb removal reduction of only 1–2%. Thus, the advantage of GOPEI with respect to unmodified GO has clearly led to the possibility of being used for the removal of both lead and arsenic ions. Removal

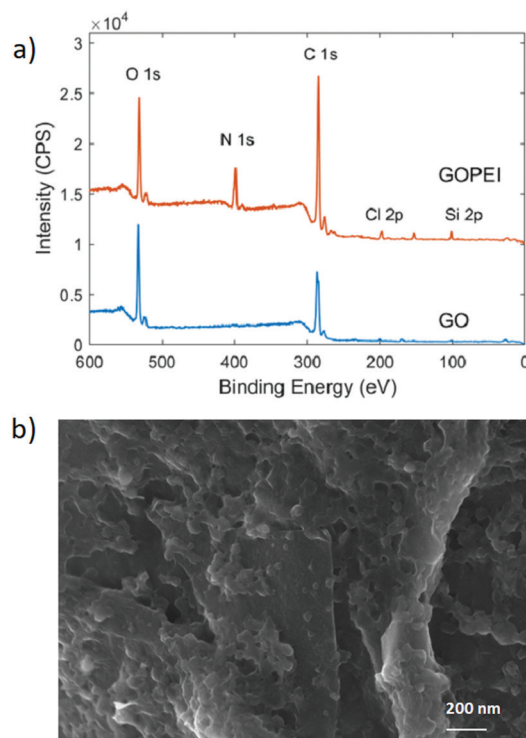


Fig. 2 (a) XPS survey spectra of pristine GO and GOPEI and (b) SEM images of GOPEI ($\text{sol. } 1 \text{ mg L}^{-1}$, sonicated for 25 min before deposition of silicon).

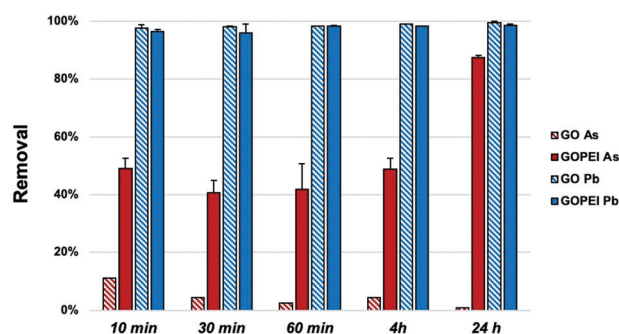


Fig. 3 As and Pb adsorption kinetics at $C_i = 100 \mu\text{L}^{-1}$ (each), ($\text{pH} = 7 \pm 0$. And solid/liquid ratio of) 13 mg/30 ml.

mechanisms of cationic heavy metals, such as Pb^{2+} , using GO are well studied and reported to depend on the great affinity towards oxygenated groups of the GO surface such as carboxyl, hydroxyl and carbonyl groups.²¹ When PEI is added, electrostatic repulsion toward positively charged ions takes over, but there is always attraction towards carboxylic groups present on the graphene, they are not fully protonated above $\text{pH} = 4$,²² which could mediate the formation of polymer-metal complexes with the amino group lone pairs (Fig. 4b).²³ Liu *et al.* stated that Pb adsorption onto fibrils conjugated with PEI was also attributed to the formation of a strong inner complex with the unquaternized N atoms of the amino groups in the PEI chains, especially at $\text{pH} > 5$.

Hence, in the case of Pb, synergetic effects of abundant functionalities in GO and complexation of polyamine are the



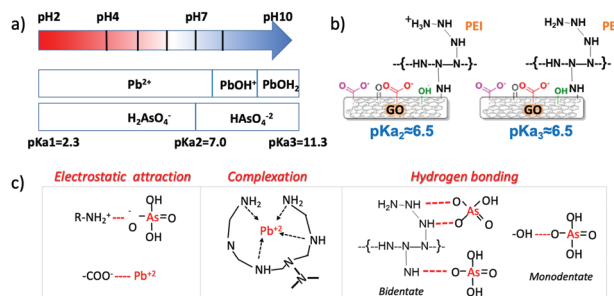


Fig. 4 (a) Contaminant (As and Pb) dominant species in the pH range of interest for water treatment. (b) Functional group protonation at the pH close to that used in this work, ²² pKa₂ refers to deprotonation of carboxylic groups in red (c) summary of the removal mechanisms driving both As and Pb adsorption according to pH conditions.

drivers for adsorption (Fig. 4). On the other hand, amine protonated groups favour anionic adsorption, as reported for the case of Cr(vi).²⁴

The anionic metal and metalloid adsorption mechanism onto PEI has been explained by both electrostatic adsorption and hydrogen bonding formation. A detailed overview of speciation of As and Pb, and functional group protonation/deprotonation *versus* pH is provided in Fig. 4 with suggested mechanisms for adsorption summarized in Fig. 4c, based on the observed data and in accordance with previously published papers.^{13,25–27}

In conclusion, GOPEI nanosheets were synthesized by a fast and easy scalable procedure involving MW assisted amination of GO and purification through hollow fiber membrane modules by microfiltration, not requiring tedious and time-consuming reiterated washing-centrifugation steps. The hollow fibers filter here proposed allowed to retain GOPEI nanosheets, wash and recover them by flow direction inversion. This procedure, never applied before for GO purification, minimizes the work-up steps generally required for modified GO purification and ensures high purity reproducibility, thanks to the standard and commercial availability of the cartridges. Altogether, these peculiarities make the MF method highly suitable for future modified-GO upscaling for real exploitation in practical applications including drinking water purification requiring high and reproducible purity. The sorption properties of MW-MF GOPEI towards two dangerous metal contaminants, lead cations and arsenic anions, simultaneously were also demonstrated. Different from unmodified GO, GOPEI nanosheets adsorbed both As and Pb ions with a removal rate higher than 90%. This was ascribed to the combined positive surface charge (promoting As interactions) and primary amine promoted complexation of Pb ions. Fixation of GOPEI on commercial point-of-use filters for drinking water purification and pilot studies will be the subject of future work.

The authors gratefully acknowledge the support of this work through the projects 825207-GO-FOR-WATER and

881603-GrapheneCore3-SH-GRAPHIL, and Dr L. Bocchi, and M. Fecondini (Medica SpA) for providing Plasmart microfiltration cartridges.

Conflicts of interest

There are no conflicts to declare.

Notes and references

- 1 C. Backes, *et al.*, *2D Mater.*, 2020, 7, 022001.
- 2 D. R. Dreyer, S. Park, C. W. Bielawski and R. S. Ruoff, *Chem. Soc. Rev.*, 2010, 39, 228–240.
- 3 S. Guo, Y. Nishina, A. Bianco and C. Ménard-Moyon, *Angew. Chem., Int. Ed.*, 2019, 59, 1542–1547.
- 4 N. Baig, M. Zambianchi, M. Sajid and T. A. Saleh, *J. Environ. Manage.*, 2019, 244, 370–382.
- 5 N. Yousefi, X. Lu, M. Elimelech and N. Tufenkji, *Nat. Nanotechnol.*, 2019, 14, 107–119.
- 6 F. Perreault, A. Fonseca de Faria and M. Elimelech, *Chem. Soc. Rev.*, 2015, 44, 5861–5896.
- 7 T. A. Tabish, F. A. Memon, D. E. Gomez, D. W. Horsell and S. Zhang, *Sci. Rep.*, 2018, 8, 1817.
- 8 L. Jiang, Y. Liu, S. Liu, G. Zeng, X. Hu, X. Hu, Z. Guo, X. Tan, L. Wang and Z. Wu, *Environ. Sci. Technol.*, 2017, 51, 6352–6359.
- 9 G. Ersan, O. G. Apul, F. Perreault and T. Karanfil, *Water Res.*, 2017, 126, 385–398.
- 10 C. J. Madadram, H. Y. Kim, G. Gao, N. Wang, J. Zhu, H. Feng, M. Goring, M. L. Kasner and S. Hou, *ACS Appl. Mater. Interfaces*, 2012, 4, 1186–1193.
- 11 M.-P. Wei, H. Chai, Y.-L. Cao and D.-Z. Jia, *J. Colloid Interface Sci.*, 2018, 524, 297–305.
- 12 C.-Z. Zhang, Y. Yuan and Z. Guo, *Sep. Sci. Technol.*, 2018, 53, 1666–1677.
- 13 A. D. Pakulski, W. Czepa, S. Witomska, A. Aliprandi, P. Pawlu, V. Patroniak, A. Ciesielski and P. Samori, *J. Mater. Chem. A*, 2018, 6, 9384–9390.
- 14 M. Zhang, K. Guan, Y. Ji, G. Liu, W. Jin and N. Xu, *Nat. Commun.*, 2019, 10, 1253.
- 15 F. Arshad, M. Selvaraj, J. Zain, F. Banat and M. Abu, *Sep. Purif. Technol.*, 2019, 209, 870–880.
- 16 S. Deng, G. Zhang, S. Chen, Y. Xue, Z. Du and P. Wang, *J. Mater. Chem. A*, 2016, 4, 15851–15860.
- 17 U. K. Chowdhury, B. K. Biswas, T. R. Chowdhury, G. Samanta, B. K. Mandal, G. C. Basu, C. R. Chanda, D. Lodh, K. C. Saha, S. K. Mukherjee, S. Roy, S. Kabir, Q. Quamruzzaman and D. Chakraborti, *Environ. Health Perspect.*, 2000, 108, 393–397.
- 18 (a) A. Kovtun, A. Bianchi and M. Zambianchi, *et al.*, *Faraday Discuss.*, 2021, DOI: 10.1039/C9FD00117D; (b) A. Kovtun, M. Zambianchi and C. Bettini, *et al.*, *Nanoscale*, 2019, 11, 22780–22787.
- 19 M. Zambianchi, A. Barbieri, A. Ventola, L. Favaretto, C. Bettini, M. Galeotti and G. Barbarella, *Bioconjugate Chem.*, 2007, 18, 1004–1009.
- 20 J. D. Ziebarth and Y. Wang, *Biomacromolecules*, 2010, 11, 29–38.
- 21 A. I. A. Sherlala, A. A. A. Raman, M. M. Bello and A. Asghar, *Chemosphere*, 2018, 193, 1004–1017.
- 22 E. S. Orth, J. G. L. Ferreira, J. E. S. Fonsaca, S. F. Blaskiewicz, S. H. Domingues, A. Dasgupta, M. Terrones and A. J. G. Zarbin, *J. Colloid Interface Sci.*, 2016, 467, 239–244.
- 23 B. Rivas, *Prog. Polym. Sci.*, 2003, 28, 173–208.
- 24 J. Geng, Y. Yin, Q. Liang, Z. Zhu and H. Luo, *Chem. Eng. J.*, 2019, 361, 1497–1510.
- 25 G. Huang, W. Li, Q. Liu, J. Liu, H. Zhang, R. Li, Z. Li, X. Jing and J. Wang, *New J. Chem.*, 2018, 42, 168–176.
- 26 F. Arshad, M. Selvaraj, J. Zain, F. Banat and M. A. Haija, *Sep. Purif. Technol.*, 2019, 209, 870–880.
- 27 S. Deng, G. Zhang, S. Chen, Y. Xue, Z. Du and P. Wang, *J. Mater. Chem. A*, 2016, 4, 15851–15860.

